

Superconducting properties of novel BiSe₂-based layered LaO_{1-x}F_xBiSe₂ single crystals

Jifeng Shao,¹ Zhongheng Liu,¹ Xiong Yao,¹ Lei Zhang,¹ Li Pi,¹ Shun Tan,¹ Changjin Zhang,^{1,*} and Yuheng Zhang¹

¹*High Magnetic Field Laboratory, Chinese Academy of Science and University of Science and Technology of China, Hefei 230026, People's Republic of China*

(Dated: submitted to EPL on May 26, 2014, revised version received July 10, 2014, accepted by EPL on July 16, 2014)

F-doped LaOBiSe₂ superconducting single crystals with typical size of 2×4×0.2 mm³ are successfully grown by flux method and the superconducting properties are studied. Both the superconducting transition temperature and the shielding volume fraction are effectively improved with fluorine doping. The LaO_{0.48}F_{0.52}BiSe_{1.93} sample exhibits zero-resistivity at 3.7 K, which is higher than that of the LaO_{0.5}F_{0.5}BiSe₂ polycrystalline sample (2.4K). Bulk superconductivity is confirmed by a clear specific-heat jump at the associated temperature. The samples exhibit strong anisotropy and the anisotropy parameter is about 30, as estimated by the upper critical field and effective mass model

PACS numbers: Valid PACS appear here

I. INTRODUCTION

Materials with layered structure have been intensively studied as a promising approach to the exploration of new high transition temperature superconductors, since the discovery of cuprate superconductors¹. This scheme has been accelerated and become much more fruitful by the discovery of the iron-based superconductors² and the following tremendous research. Both the cuprate and iron-based superconductors have a layered structure consisting of the so-called superconducting layers (CuO₂ layer, Fe₂M₂(M=As, P, S, Se or Te)layer) and the blocking charge reservoir layers^{3,4}. Superconductivity occurs when charge carriers are generated in the charge reservoir layers and transferred into the superconducting layers. By changing the blocking layers or intercalating some molecular space layers, a lot of derivative superconductors with the same superconducting layers are discovered^{5,6}.

Recently, novel BiS₂-based superconductivity has been reported in layered compound Bi₄O₄S₃⁷, which is composed of Bi₂O₂(SO₄)_(1-x) (x=0.5) blocking layers and BiS₂ superconducting layers. Subsequently, an analogous series of BiS₂-based superconductors are discovered, including ReO_{1-x}F_xBiS₂ (Re= La, Ce, Nd, Yb, Pr)⁸⁻¹², La_{1-x}M_xOBiS₂ (M= Ti, Zr, Hf, Th)¹³, and Sr_{1-x}La_xFBiS₂^{14,15}, ect. The transition temperature of the BiS₂-based superconductors can be as high as 10.6 K^{8,16}. These reports suggest that it is possible to discover more BiS₂-derivative superconducting materials. Very recently, superconductivity with transition temperature of 2.4 K has been reported in LaO_{0.5}F_{0.5}BiSe₂ polycrystalline sample¹⁷. This discovery is of great importance since it represents a novel BiSe₂-based superconducting system. However, due to the lack of single crystal, the superconducting properties remain to be investigated. In this paper, we report the successful growth of LaO_{1-x}F_xBiSe₂ single crystal samples by flux method. The superconducting parameters are determined based on the high-quality single crystals.

II. EXPERIMENT

The LaO_{1-x}F_xBiSe₂ single crystals were grown by flux method using a mixture of CsCl and KCl as the flux (the molar ratio of CsCl : KCl is 5 : 3)¹⁸⁻²¹. The starting materials of high-purity Bi₂O₃, BiF₃, Bismuth, Lanthanum and Selenium were weighed with nominal concentrations of LaO_{1-x}F_xBiSe₂ and thoroughly ground in an agate mortar. Then the flux of CsCl and KCl were added, with the mass ratio of CsCl/KCl to raw materials of 1 : 8. The total mixture was thoroughly ground and then sealed in an evacuated quartz tube. It was slowly heated to 800 °C and kept for 48 h followed by cooling down at a rate of 2 K/h to 560 °C before the furnace was shut down. After cooling down to the room temperature, the product was removed from the quartz tube and washed by distilled water to get the single crystal samples.

The real compositions of the obtained single crystals were determined by an energy dispersive x-ray spectroscopy (EDX) analysis, which was performed using Oxford SWIFT3000 spectroscopy equipped with a Si detector. The EDX measurement were done on several pieces of single crystals randomly selected from each sample. For each piece, at least six different points were randomly selected in the EDX measurements and the average was defined as the actual composition. The structure of the obtained crystal was characterized by powder and single crystal x-ray diffraction with Cu-K_α at room temperature. The temperature dependence of resistivity from 2 K to 300 K was measured by a standard four-probe method in a commercial Quantum Design physical property measurement system (PPMS-14 T) system. Magnetic properties were performed using a superconducting quantum interference device magnetometer. The specific heat measured by a thermal relaxation method from 20 K down to 1.9 K was also performed on PPMS-14 T system.

TABLE I. The comparison between nominal and real compositions of different F-doped $\text{LaO}_{1-x}\text{F}_x\text{BiSe}_2$ single crystals, determined by EDX.

Nominal composition	Measured chemical composition
$\text{LaO}_{0.8}\text{F}_{0.2}\text{BiSe}_2$	$\text{LaO}_{0.63}\text{F}_{0.37}\text{Bi}_{1.00}\text{Se}_{1.92}$
$\text{LaO}_{0.7}\text{F}_{0.3}\text{BiSe}_2$	$\text{LaO}_{0.62}\text{F}_{0.38}\text{Bi}_{1.00}\text{Se}_{1.92}$
$\text{LaO}_{0.5}\text{F}_{0.5}\text{BiSe}_2$	$\text{LaO}_{0.59}\text{F}_{0.41}\text{Bi}_{0.99}\text{Se}_{1.92}$
$\text{LaO}_{0.3}\text{F}_{0.7}\text{BiSe}_2$	$\text{LaO}_{0.54}\text{F}_{0.46}\text{Bi}_{0.99}\text{Se}_{1.93}$
$\text{LaO}_{0.1}\text{F}_{0.9}\text{BiSe}_2$	$\text{LaO}_{0.48}\text{F}_{0.52}\text{Bi}_{1.00}\text{Se}_{1.93}$

III. RESULTS AND DISCUSSION

Figure 1 shows the scanning electron microscopy photograph of the $\text{LaO}_{0.59}\text{F}_{0.41}\text{BiSe}_{1.92}$ sample. The obtained single crystal samples have typical dimensions of $2 \times 4 \times 0.2 \text{ mm}^3$. In order to determine the actual compositions of the samples we perform an energy-dispersive x-ray spectrometry (EDX) analysis on the as-grown single crystals. The results are given in Table 1. The obtained values are normalized by $\text{La} = 1$, and the oxygen content is defined as $1-x$ (x is the content of F), considering the inaccuracy of oxygen by EDX measurement. No Cs, K, and Cl elements are detected in the samples. For La, Bi and Se elements, the relative ratio agrees well with the stoichiometric ratio except for a little deficiency of Se, which is similar to the deficiency of S in $\text{NdO}_{1-x}\text{F}_x\text{BiS}_2$ single crystals²². It can be seen that the actual F concentration increases with increasing nominal F content. However, the actual F content saturates at about 0.5 (for example, the actual F content is $x=0.52$ in the sample with nominal content of $x=0.9$). Another noticeable fact is that for the samples with nominal contents $x=0.2$ and $x=0.3$, the actual F contents are about 0.37 and 0.38, which are significantly higher than the nominal contents. These results indicate that in the $\text{LaO}_{1-x}\text{F}_x\text{BiSe}_2$ single crystals, the preferred F content is in the $x=0.3-0.6$ region. Similar results have also been discovered in $\text{LaO}_{1-x}\text{F}_x\text{BiS}_2$ single crystals²³.

Figure 2(a) gives the powder x-ray diffraction (XRD) pattern of the $\text{LaO}_{0.59}\text{F}_{0.41}\text{Bi}_{0.99}\text{Se}_{1.92}$ sample and the refinement on the XRD pattern. The sample has a $P4/nmm$ tetragonal lattice with lattice constants $a=4.1377 \text{ \AA}$ and $c=14.1566 \text{ \AA}$. The atom coordinates and site occupancy determined from the Rietveld refinement ($R_{wp} = 3.27\%$) are also given in Fig. 2(a). A schematic image of the crystal structure is plotted in Fig. 2(b). Figure 2(c) shows the single crystal XRD patterns of the samples. Only (00ℓ) diffraction peaks are observed, confirming that the samples are all single crystals and the crystallographic c -axis is perpendicular to the shining surface. Figure 2(d) shows the shift of the (004) diffraction peaks with increasing F content. The (004) peak shifts toward higher angle as the F content increases from 0.38 to 0.52. Accordingly, the calculated c -axis lattice parameter decreases from 14.1642 \AA to 14.0024 \AA . The slight shrinkage of the c -axis lattice parameter is reason-

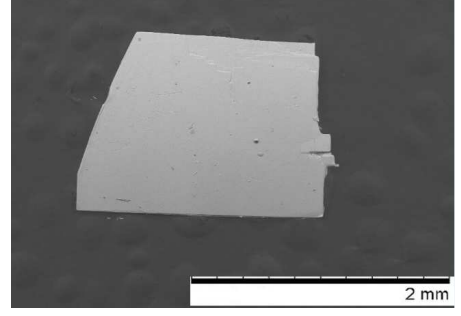


FIG. 1. The SEM photograph of an as-grown F-doped LaOBiSe_2 single crystal.

TABLE II. The comparison of the lattice parameters and the transition temperatures between the polycrystalline (P) and single crystal (S) samples of $\text{LaO}_{0.5}\text{F}_{0.5}\text{BiSe}_2$ and $\text{LaO}_{0.5}\text{F}_{0.5}\text{BiS}_2$.

Compound	a (Å)	c (Å)	T_c^{zero} (K)	$T_c^{\text{susceptibility}}$ (K)
$\text{LaO}_{0.5}\text{F}_{0.5}\text{BiSe}_2\text{-P}$	4.15941	14.01567	2.4	2.6
$\text{LaO}_{0.48}\text{F}_{0.52}\text{BiSe}_2\text{-S}$	4.15663	14.0024	3.7	3.7
$\text{LaO}_{0.5}\text{F}_{0.5}\text{BiS}_2\text{-P}$	4.0527	13.3237	2.5	2.7
$\text{LaO}_{0.54}\text{F}_{0.46}\text{BiS}_2\text{-S}$...	13.39	3.0	3.0

able because the ionic radius of F^- is smaller than that of O^{2-} .

Figure 3(a) shows the temperature dependence of resistivity of the $\text{LaO}_{1-x}\text{F}_x\text{BiSe}_2$ single crystals. The samples exhibit a metallic-like behavior at normal state, which is consistent with the $\text{LaO}_{0.5}\text{F}_{0.5}\text{BiSe}_2$ polycrystalline samples¹⁷. The superconducting transition occurs at low temperature for all samples. For the $x=0.52$ sample, the T_c^{onset} value is about 4.2 K and the T_c^{zero} is 3.7 K, which are much higher than those of $\text{LaO}_{0.5}\text{F}_{0.5}\text{BiSe}_2$ polycrystalline sample. Both the T_c^{onset} and T_c^{zero} values shift toward lower temperature as the F doping content decreases, which is shown in the inset of Fig. 3(a). For all samples, the superconducting transition width is less than 0.5 K, suggesting the high quality of the single crystals. In order to investigate the superconducting properties under magnetic field, we perform the resistivity versus temperature measurements at different applied magnetic field. The results for $H\parallel ab$ and $H\parallel c$ are shown in Figs. 3(b) and (c), respectively. It can be seen that the T_c^{onset} value decreases and the superconducting transition width becomes larger with increasing applied magnetic field, indicating that the superconducting state is suppressed by applying magnetic field. It can also be seen that the suppression effect is much faster in the $H\parallel c$ case than that in the $H\parallel ab$ case. To estimate the upper

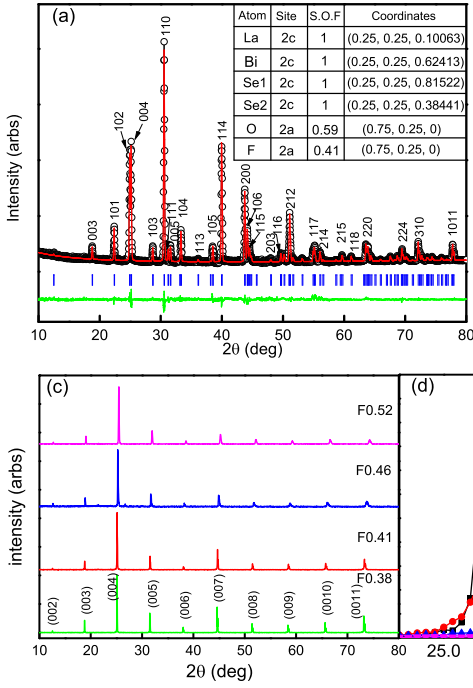


FIG. 2. (color online) (a) X-ray diffraction patterns of different F-doped $\text{LaO}_{1-x}\text{F}_x\text{BiSe}_2$ single crystals. (b) XRD pattern of (004) diffraction peaks for $\text{LaO}_{1-x}\text{F}_x\text{BiSe}_2$ single crystals. (c) Crystal structure of $\text{LaO}_{0.5}\text{F}_{0.5}\text{BiSe}_2$ derived by replacement of S by Se in the known $\text{LaO}_{0.5}\text{Bi}_{0.5}\text{S}_2$ structure. The orthogon indicates the unit cell.

critical fields of the $\text{LaO}_{0.48}\text{F}_{0.52}\text{BiSe}_{1.93}$ sample along different direction, we plot the field dependence curves of the T_c^{onset} and T_c^{zero} values for the $H\parallel ab$ and $H\parallel c$ cases. The results are shown in the insets of Figs. 3(b) and (c), respectively. The irreversible field $\mu_0 H_{irr}(0)$ is estimated to be about 5.4 T and 0.4 T for the $H\parallel ab$ and $H\parallel c$ cases, respectively. The upper critical field at zero temperature is estimated to be 29 T and 1 T for the $H\parallel ab$ and $H\parallel c$ cases, as determined by the Werthamer-Helfand-Hohenberg (WHH) theory²⁴:

$$\mu_0 H_{c2}(0) = -0.69 T_c (d\mu_0 H_{c2}/dT)_{T_c}. \quad (1)$$

The anisotropy parameter is preliminary evaluated to be 33.3 using the equation:

$$\gamma_s = \frac{dH_{c2}^{\parallel ab}/dT}{dH_{c2}^{\parallel c}/dT}. \quad (2)$$

Figure 3(d) shows the temperature dependence of magnetic susceptibility measured under zero-field-cooling (ZFC) and field-cooling (FC) processes for the $\text{LaO}_{1-x}\text{F}_x\text{BiSe}_2$ samples. The applied field is parallel to the ab -plane. Large diamagnetic signal is observed in all samples, confirming the occurrence of superconductivity. The diamagnetic signal is enhanced with increasing F content. We calculate the shielding volume fraction (SVF) using the formula $\text{SVF} = 4\pi\chi\rho/H$ (ρ is the

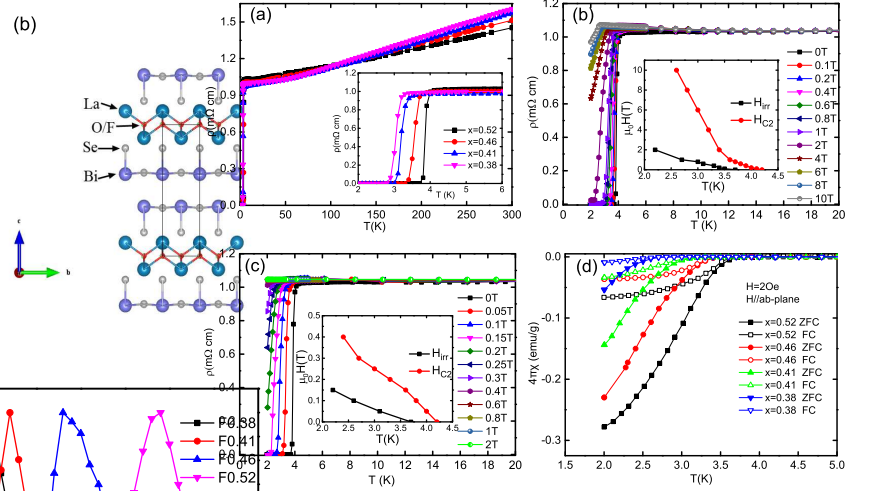


FIG. 3. (color online) (a) Temperature dependence of resistivity of $\text{LaO}_{1-x}\text{F}_x\text{BiSe}_2$ single crystals from 2K to 300K. The inset shows an enlarge of superconducting transition. (b) and (c) Temperature dependence of resistivity of $\text{LaO}_{0.48}\text{F}_{0.52\pm 0.01}\text{Bi}_{1.00\pm 0.01}\text{Se}_{1.93\pm 0.03}$ single crystal under zero and different magnetic fields of (b) $H\parallel ab$ -plane and (c) $H\parallel c$ -axis. The inset of (b) and (c) shows temperature dependence of the upper critical field H_{c2} , and H_{irr} , determined from T_c^{Onset} and T_c^{Zero} . (d) Temperature dependence of magnetic susceptibility under ZFC and FC processes for $\text{LaO}_{1-x}\text{F}_x\text{BiSe}_2$ single crystals. The applied magnetic field is 20Oe, parallel to ab -plane.

mass density of the sample and H is the applied magnetic field). For the $\text{LaO}_{0.48}\text{F}_{0.52}\text{BiSe}_{1.93}$ sample, the estimated SVF is almost 100% at 2K, confirming the occurrence of bulk superconductivity. Table 2 gives a comparison on the lattice constants and the superconducting transitions between the polycrystalline and single crystal of $\text{LaO}_{0.5}\text{F}_{0.5}\text{BiSe}_2$ and $\text{LaO}_{0.5}\text{F}_{0.5}\text{BiS}_2$ samples. It can be seen that the single crystal samples have higher superconducting transition temperature.

In order to scale the anisotropy parameter (γ_s) of the single crystal samples, we measure the angular (θ) dependence of resistivity of the $\text{LaO}_{0.48}\text{F}_{0.52}\text{BiSe}_{1.93}$ sample under various applied magnetic fields at a fixed temperature of 3 K. The results are shown in Fig. 4(a). Here θ is defined as the angular between ab -plane and the direction of the applied magnetic field. According to Ginzburg-Landau theory, the curves of ρ versus reduced magnetic field (H_{red}) under various applied magnetic fields should be fitted to one²⁵. The reduced magnetic field is given by $H_{red} = H(\sin^2\theta + \gamma_s^{-2}\cos^2\theta)^{1/2}$. As the $H_{c2}^{\parallel c}$ value for the $\text{LaO}_{0.48}\text{F}_{0.52}\text{BiSe}_{1.93}$ sample is about 1 T, we adopt the data taken from the 0-1 T range to make the fit for γ_s . The result is shown in Fig. 4(b). The anisotropy parameter γ_s at 3K is about 30, which is close to the preliminary evaluated value of 33.3.

In order to confirm the occurrence of bulk superconductivity, we measure the specific heat for the

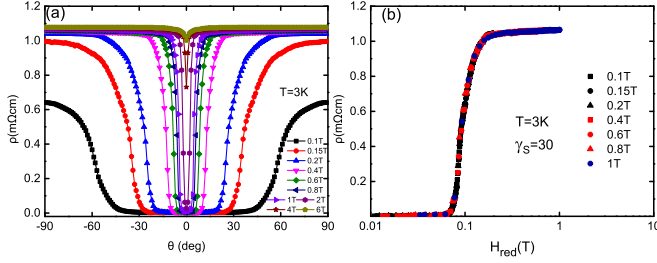


FIG. 4. (color online) (a) Angular dependence of resistivity of $\text{LaO}_{0.48}\text{F}_{0.52\pm0.01}\text{Bi}_{1.00\pm0.01}\text{Se}_{1.93\pm0.03}$ single crystal under different magnetic field from 0.1T up to 6T at fixed temperature 3K. Here, the angle θ is defined as the angle between the ab -plane and the magnetic direction. (b) Scaling of the resistivity versus the reduced magnetic field $H_{red} = H(\sin^2\theta + \gamma_s^{-2}\cos^2\theta)^{1/2}$ at 3K in different magnetic field from 0.1T to 1T.

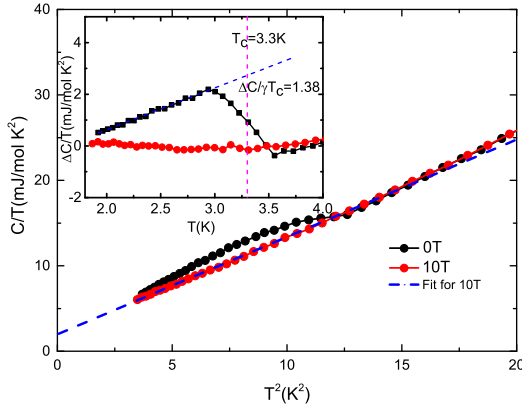


FIG. 5. (color online) Temperature dependence of specific heat C at superconducting state (0T) and normal state (10T) for $\text{LaO}_{0.54}\text{F}_{0.46\pm0.01}\text{Bi}_{0.99\pm0.02}\text{Se}_{1.93\pm0.02}$ single crystal, plotted in the form of C/T versus T^2 . The dashed line is the fit to the normal state at low temperature. The inset shows temperature dependences of the difference in the electronic specific heat between the superconducting state and the normal state by subtracting the phononic contribution, $C_e = C(0T) - C(10T)$.

$\text{LaO}_{0.54}\text{F}_{0.46}\text{BiSe}_{1.93}$ single crystal from 1.9 K to 20 K. In general, the specific heat value at low temperature is very small. Thus we select the $\text{LaO}_{0.54}\text{F}_{0.46}\text{BiSe}_{1.93}$ sample ($T_c^{\text{zero}} = 3.3$ K) to perform the measurement because

we can get relatively large size of $\text{LaO}_{0.54}\text{F}_{0.46}\text{BiSe}_{1.93}$ single crystals comparing to other samples. The temperature dependence of specific heat in the superconducting state ($H=0$ T) and normal state ($H=10$ T) is plotted in Fig. 5. A clear specific-heat jump occurs at about 3.3 K, confirming the occurrence of bulk superconductivity. According to the relation of $C/T = \gamma + \beta T^2$, we fit the normal state data to a polynomial. The best fitting results suggest that the normal state electronic-specific-heat coefficient γ and lattice coefficient β are 1.97 mJ/mol K² and 1.14 mJ/mol K², respectively. As the phononic contribution (βT^2) is usually independent on applied magnetic field, we get the electronic specific heat by $C_e = C(0\text{ T}) - C(10\text{ T})$. The inset of Fig. 5 shows the temperature dependence of electronic specific heat in the normal and superconducting state. The electronic specific heat jump at transition temperature (3.3 K) is evaluated to be $\Delta C_e / \gamma T_c = 1.38$. The estimated value of $\Delta C_e / \gamma T_c$ is comparable to the Bardeen-Cooper-Schrieffer weak-coupling limit value 1.43. As the specific heat at the superconducting state is a little higher than that of normal state, ultra low temperature data is needed to study the mechanism of $\text{LaO}_{1-x}\text{F}_x\text{BiSe}_2$ superconductors.

IV. CONCLUSION

In summary, we report the successful growth of $\text{LaO}_{1-x}\text{F}_x\text{BiSe}_2$ superconducting single crystals for the first time. F doping can substantially enhance the superconducting transition temperature and the shielding volume fraction. The highest $T_c^{\text{zero}} \sim 3.7$ K and almost 100% shielding volume fraction are obtained in the $\text{LaO}_{0.48}\text{F}_{0.52}\text{BiSe}_{1.93}$ sample. The single crystal samples exhibit strong anisotropy and the anisotropy parameter is estimated to be about 30. The upper critical fields parallel to the c -axis and the ab -plane are evaluated to be 1 T and 29 T, respectively. We also confirm the bulk superconductivity of the $\text{LaO}_{1-x}\text{F}_x\text{BiSe}_2$ samples by specific heat measurement.

V. ACKNOWLEDGMENTS

This work was supported by the State Key Project of Fundamental Research of China (Grant Nos. 2010CB923403 and 2011CBA00111), the Nature Science Foundation of China (Grant Nos. 11174290 and U1232142).

* zhangcj@hmf.ac.cn

¹ J. G. Bednorz and K. A. Muller, Phys. B **64**, 189 (1986).

² Y. Kamihara, T. Watanabe, M. Hirano, and H. Hosono, J. Am. Chem. Soc. **130**, 3296 (2008).

³ G. R. Stewart, Rev. Mod. Phys. **83**, 1589 (2011).

⁴ K. Ishida, Y. Nakai, and H. Hosono, J. Phys. Soc. Jpn. **78**, 062001 (2009).

⁵ M. Burrard-Lucas, D. G. Free, S. J. Sedlmaier, J. D. Wright, S. J. Cassidy, Y. Hara, A. J. Corkett, T. Lancaster, P. J. Baker, S. J. Blundell and S. J. Clarke, Nat. Mater. **12**, 15 (2013).

- ⁶ T. Hatakeda, T. Noji, T. Kawamata, M.Kato, and Y. Koike, J. Phys. Soc. Jpn. **82**, 123705 (2013).
- ⁷ Y. Mizuguchi, H. Fujihisa, Y. Gotoh, K. Suzuki, H. Usui, K. Kuroki, S. Demura, Y. Takano, H. Izawa, and O. Miura, Phys. Rev. B **86**, 220510 (2012).
- ⁸ Y. Mizuguchi, S. Demura, K. Deguchi, Y. Takano, H. Fujihisa, Y. Gotoh, H. Izawa, and O. Miura, J. Phys. Soc. Jpn. **81**, 114725 (2012).
- ⁹ R. Jha, A. Kumar, S. K. Singh, and V. P. S. Awana, J. Supercond. Nov. Mag. **26**, 499 (2013).
- ¹⁰ R. Jha, A. Kumar, S. K. Singh, and V. P. S. Awana, J. Appl. Phys. **113**, 056102 (2013).
- ¹¹ J. Xing, S. Li, X. Ding, H. Yang, and H. H. Wen, Phys. Rev. B. **86**, 214518 (2012).
- ¹² D. Yazici, K. Huang, B. D. White, A. H. Chang, A. J. Friedman, and M. B. Maple, Philos. Mag. **93**, 673 (2012).
- ¹³ D. Yazici, K. Huang, B. White, I. Jeon, v. Burnett, A. Friedman, I. Lum, I. Nallaiyan, S. Spagna and M. Maple, Phys. Rev. B. **87**, 174512 (2013).
- ¹⁴ X. Lin, X. Ni, B. Chen, X. Xu, X. Yang, J. Dai, Y. Li, X. Yang, Y. Luo, Q. Tao, G. Cao, and Z. Xu, Phys. Rev. B. **87**, 020504 (2013).
- ¹⁵ H. Sakai, D. Kotajima, K. Saito, H. Wadati, Y. Wakisaka, M. Mizumaki, K. Nitta, Y. Tokura, and S. Ishiwata, J. Phys. Soc. Jpn. **83**, 014709 (2014).
- ¹⁶ C. T. Wolowiec *et al.*, Phys. Rev. B **88**, 064503 (2013).
- ¹⁷ A. Krzton-Maziopa, Z. Guguchia, E. Pomjakushina, V. Pomjakushin, R. Khasanov, H. Luetkens, P. Biswas, A. Amato, H. Keller, and K. Conder, J. Phys.: Condens. Matter **26**, 215702 (2014).
- ¹⁸ M. Masaoka and A. Kyono, Mater. Lett. **60**, 3922 (2006).
- ¹⁹ R. Hu, H. Lei, M. Abeykoon, E. S. Bozin, S. J. L. Billinge, J. B. Warren, T. Siegrist, and C. Petrovic, Phys. Rev. B. **83**, 224502 (2011).
- ²⁰ G. N. Oh and J. A. Ibers, Acta Cryst. E **67**, i75 (2011).
- ²¹ M. Nagao, S. Demura, K. Deguchi, A. Miura, S. Watauchi, T. Takei, Y. Takano, N. Kumada, and I. Tanaka, J. Phys. Soc. Jpn. **82**, 113701 (2013).
- ²² J. Liu, D. Fang, Z. Wang, J. Xing, Z. Du, X. Zhu, H. Yang, and H. H. Wen, arXiv:1310.0377.
- ²³ M.Nagao, A. Miura, S. Demura, K. deguchi, S. Watauchi, T. Takei, Y. Takano, N. Kumada, and I. Tnaka, Solid State Commun. **178**, 33 (2014).
- ²⁴ N. R. Werthamer, E. Helfand, and P. C. Hohenberg, Phys. Rev. B.**147**, 295 (1966).
- ²⁵ G. Blatter, V. B. Geshkenbein, and A. I. Larkin, Phys. Rev. L.**68**, 875 (1992).